LBL-32832
UC-404

Lawrence Berkeley Laboratory
UNIVERSITY OF CALIFORNIA

Materials Sciences Division

Presented at the 91st Annual Conference of the Deutsche Bunsen-Gesellschaft für Physikalische Chemie, Vienna, Austria, May 28–30, 1992, and to be published in the Proceedings

Towards a First-Principles Thermodynamics of Solids

D. de Fontaine and C. Wolverton

August 1992

REFERENCE COPY
Does Not
Circulate
LBL-32832
Copy 1
Bldg. 50 Library.

Prepared for the U.S. Department of Energy under Contract Number DE-AC03-76SF00098

DISCLAIMER

This document was prepared as an account of work sponsored by the United States Government. While this document is believed to contain correct information, neither the United States Government nor any agency thereof, nor the Regents of the University of California, nor any of their employees, makes any warranty, express or implied, or assumes any legal responsibility for the accuracy, completeness, or usefulness of any information, apparatus, product, or process disclosed, or represents that its use would not infringe privately owned rights. Reference herein to any specific commercial product, process, or service by its trade name, trademark, manufacturer, or otherwise, does not necessarily constitute or imply its endorsement, recommendation, or favoring by the United States Government or any agency thereof, or the Regents of the University of California. The views and opinions of authors expressed herein do not necessarily state or reflect those of the United States Government or any agency thereof or the Regents of the University of California.

LBL-32832
UC-404

Towards a First-Principles Thermodynamics of Solids

D. de Fontaine

Department of Materials Science and Mineral Engineering
University of California
and
Materials Sciences Division
Lawrence Berkeley Laboratory
University of California
Berkeley, CA 94720

and

C. Wolverton

Department of Physics
University of California
and
Materials Sciences Division
Lawrence Berkeley Laboratory
University of California
Berkeley, CA 94720

August 1992

This work was supported by the Director, Office of Energy Research, Office of Basic Energy Sciences, Materials Sciences Division, of the U.S. Department of Energy under Contract No. DE-AC03-76SF00098.

TOWARDS A FIRST-PRINCIPLES THERMODYNAMICS OF SOLIDS

D. de Fontaine
Department of Materials Science and Mineral Engineering, University of California, Berkeley, CA 94720, USA
Materials Sciences Division, Lawrence Berkeley Laboratory, Berkeley, CA 94720, USA
and
C. Wolverton
Department of Physics, University of California, Berkeley, CA 94720, USA
Materials Sciences Division, Lawrence Berkeley Laboratory, Berkeley, CA 94720, USA

Abstract

Total energy density-functional methods have made it possible to calculate, from first principles, such important properties as cohesive energies, lattice constants and elastic moduli for elemental crystals and perfectly ordered compounds. Real solids are imperfect, however, so that lattice vibrations and compositional disorder lead to entropy contributions, vibrational and configurational. When these effects are included in an appropriate manner, properties of real crystals can be computed *ab initio* as a function of temperature and concentration. Consequently, it is possible to obtain, virtually from the knowledge of atomic numbers alone, such basic thermodynamic properties as free energies, entropies, heats of formation, and lattice parameters for stable and metastable phases, leading, for example, to the successful computation of certain classes of phase diagrams. Recent progress in the field will be reviewed.

1. Introduction

It was in 1951 that the Cluster Variation Method (CVM) was introduced by Ryoichi Kikuchi [1]. In the following years, CVM calculations were performed, in particular by Kikuchi himself, mainly for the purpose of improving on the values of critical temperatures for various two- and three-dimensional Ising models. An important breakthrough occurred in 1973 when van Baal [2] first applied the CVM to the calculation of an ordering phase diagram of a model binary alloy on an fcc lattice. A realistic Cu-Au phase diagram was shortly thereafter calculated by Kikuchi and the present author [3], in which the energy parameters, first neighbor pair and tetrahedron interactions, were obtained by fitting to the experimentally determined phase diagram.

First neighbor pair ordering on the fcc lattice in a binary (A,B) system presents a special challenge because of the phenomenon of *frustration*: on an nn (nearest neighbor) triangle, a basic geometrical feature of the fcc lattice, all three atomic pairs cannot all satisfy the requirement of unlike (A-B) pair bonds. The Bragg-Williams model, which contains no geometrical information, cannot deal with frustration, but the CVM handles the problem very well. Unfortunately, the complexity of ordering reactions which can occur cannot be modeled by nn interactions alone; at the very least, second neighbors (nnn) must be included. It was therefore necessary to go beyond the nn tetrahedron cluster approximation in the CVM. The tetrahedron-octahedron combination was found to be a suitable CVM approximation incorporating nnn interactions [4], and a series of "prototype phase diagrams" was calculated in this T-O approximation for varying ratios of the values of the nn to nnn pair interactions [4-7]. Surprisingly, these calculations were the first ever to describe phase equilibrium on the fcc lattice for nn and nnn interactions. It is remarkable that such an apparently simple and classical problem had to wait this long for a solution, a solution made possible by the development of the CVM, its application to phase diagram calculations, the derivation of the T-O approximation, and the availability of fast computers. Moreover, by these calculations, it was shown how very different phase diagrams, with different ordered superstructures could be made to evolve continuously from one another, all the way to miscibility gap behavior, simply by changing the value of a single dimensionless parameters, the ratio of nn and nnn pair interactions.

Realistic phase diagrams, reproducing the crystalline phase boundaries observed in real binary systems, further required the introduction into the CVM free energy of either concentration-dependent interactions or of multi-site interactions. Quite impressive results could be obtained by fitting, as was done by Sigli and Sanchez for the Al-Li phase diagram [8], for example, but it was far more satisfying to try to calculate the required parameters from physical principles, ideally from first principles, i.e., from the mere knowledge of the atomic numbers Z_A, Z_B of the constituents.

To achieve this ambitious but exciting goal, it was necessary to establish a link between quantum and statistical aspects of the problem. The connection turned out to be based on the

clusters of the CVM, thanks to a remarkable orthogonal property of "cluster functions", already discovered by Sanchez in the late seventies [4], and formulated rigorously by himself, Ducastelle and Gratias in a classic paper of 1984 [9]. The key result of this work was that any function depending on atomic configurations could be rigorously expanded in a set of complete, orthonormal cluster functions, with expansion coefficients given by generalized scalar products over the space of configurations.

The basic idea of the method will be briefly described in Section 2 (for details, the reader is referred to the cited literature), then applied to the problem of determining effective cluster interactions (Section 3), to that of calculating ground states (Section 4), and to phase diagram calculations (Section 5). Examples of calculations pertaining to Pd, Rh, and V alloys will be given in Section 6.

2. Cluster Method

The cluster method works best on perfect lattices, i.e., on crystals for which we may associate an atom uniquely to each lattice (or sublattice) point. It does not mean that atomic displacements are disallowed, but merely that the *reference* lattice is unbroken, undistorted. Hence, we are considering only compositional, not topological disorder. That being the case, it becomes possible to decouple configurational from vibrational entropy. The CVM does very well for the former, is not particularly appropriate for the latter.

In binary alloys (A,B), we may then associate the value $\sigma = +1$ (A atom) or $\sigma = -1$ (B atom) to each lattice point. A *configuration* is then an N-dimensional vector σ consisting of +1 and –1 values, N being the total number of lattice points. Of course, +1 may also represent an atom A, –1 a vacancy. A binary alloy with vacancies must be modeled as a ternary system, etc.

Such an explicit description of configuration is neither practical nor useful. In the past, "configuration" was characterized somewhat ambiguously by long-range and short-range order parameters. A more general and straightforward definition is based on the notion of clusters, consisting of small collections of lattice points: pairs, triplets, quadruplets, and so on. Let α

denote such a cluster of lattice points $\{p_1, p_2, \ldots p_n\}$ and define a corresponding cluster function which we define, at least for the time being, as the product of σ's on the cluster points:

$$\varphi_\alpha(\sigma) \equiv \sigma_{p_1}\sigma_{p_2}\ldots\sigma_{p_\alpha} \tag{1}$$

The following *orthogonality*

$$<\varphi_\alpha(\sigma), \varphi_\beta(\sigma)> = \delta_{\alpha\beta} \tag{2}$$

and *completeness*

$$\sum_\alpha \varphi_\alpha(\sigma)\,\varphi_\alpha(\sigma') = \delta(\sigma, \sigma') \tag{3}$$

relations can be proved [9,11], where the angle brackets denote an inner product over the space of configurations, thus a normalized trace (or sum) over all 2^N possible configurations (for a binary system).

From this important property, it follows that any function of configuration $f(\sigma)$ can be expanded in a set of cluster functions

$$f(\sigma) = \sum_\alpha F_\alpha\,\varphi_\alpha(\sigma) \tag{4}$$

with coefficients obtained by the "inversion formula"

$$F_\alpha = <\varphi_\alpha(\sigma), f(\sigma)> \quad . \tag{5}$$

The thermodynamic, or ensemble average of $f(\sigma)$ is also of interest, it is given by

$$\bar{f} = \sum_{\alpha} F_{\alpha} \xi_{\alpha} \tag{6}$$

where the cluster, or multisite *correlation function* is given by

$$\xi_{\alpha} = \overline{\varphi_{\alpha}(\sigma)} \tag{7}$$

where the super-bar in Eqs. (6) and (7), and elsewhere, denotes thermodynamic average. Since the expansion coefficients F_{α} are obtained in Eq. (5) by performing a sum over all possible configurations, they must not depend on the average concentration $c = (1 - \bar{\sigma})/2$ of B atoms ($\bar{\sigma}$ is the average "spin" variable over all N points).

There is another way of defining scalar products, that is to perform summations over those configurations which conserve the average concentration c. It can be shown [10], in that case, that the required set of orthonormal functions differs slightly from that of cluster functions, as defined by Eq. (1): one must now take

$$\widehat{\varphi_{\alpha}}(\sigma) = \prod_{p} (\sigma_p - \bar{\sigma}) \tag{8}$$

where the product must be taken over points p of the cluster α. Correspondingly, the ensemble average of the modified cluster functions $\widehat{\varphi_{\alpha}}$ are multisite *cumulants*

$$\widehat{\xi_{\alpha}} = \overline{\prod_{p} (\sigma_p - \bar{\sigma})} \tag{9}$$

rather than correlation functions. In Eqs. (8), (9) and following, a caret denotes quantities related to c-dependent summations.

In this restricted-summation scheme, the expansion coefficients $\widehat{F_{\alpha}}$ are necessarily concentration dependent. Both types of expansions, unrestricted or restricted, are valid, indeed are

equally rigorous. The cumulant for cluster α may be expressed as a function of correlations of subcluster of α (denoted symbolically as "$\alpha - 1$", "$\alpha - 2$", ...)

$$\widehat{\xi_\alpha} = \xi_\alpha - \xi_{\alpha-1}\bar{\sigma} + \xi_{\alpha-2}\bar{\sigma}^2 \ldots \tag{10}$$

When such expressions are introduced into a concentration-dependent expansion for the expectation value (ensemble average) of some function f, and when the two equivalent expansions, concentration-independent and -dependent, are compared term for term, a simple relationship is found between the coefficients F_α and $\widehat{F_\beta}$ [10]. The former can be expressed linearly as a function of the latter and of powers of $\bar{\sigma}$. Surprisingly, the explicit concentration-dependence of the $\bar{\sigma}$ compensates for the implicit concentration-dependence of the $\widehat{F_\beta}$ to produce the concentration-independent F_α. These considerations are particularly relevant to the case of expansions of the energy in terms of *effective cluster interactions*, to be taken up next.

3. Effective Cluster Interactions

Let us expand the energy $E(\sigma)$ of a given configuration, as in Eq. (4). The expansion coefficients are obtained by the inversion formula (5). To illustrate how this calculation is to be performed, consider the case $\alpha = (p,q)$, i.e., a cluster consisting of a pair of atoms situated at lattice points p and q. We split the sum over configurations into two contributions: a sum over cluster (pair) configurations and one over σ', consisting of all configurations of the "medium" on lattice points not including p, q. We find

$$E_{pq} = \frac{1}{2^2}\sum_{\sigma_p}\sum_{\sigma_q}\sigma_p\sigma_q\left[2^{N-2}\sum_{\sigma'}E(\sigma_p,\sigma_q;\sigma')\right] \tag{11}$$

or, since each σ can be ± 1,

$$E_{pq} = \tfrac{1}{4}(W_{AA} + W_{BB} - W_{AB} - W_{BA}) \tag{12}$$

where W_{IJ} (I, J = A or B) is the average energy of all configurations having atom of type I at p and J at q. Similar expressions can be derived rigorously for triplets p, q, r:

$$E_{pqr} = \tfrac{1}{8}(W_{AAA} - W_{AAB} \cdots + W_{BBB}) \quad ,$$

quadruplets, etc. The E_α are the effective cluster interactions (ECI) mentioned above, and are obtained as (small) differences of (large) total energies, W. These effective interactions, the correct ones to use in Ising-model-like calculations, differ fundamentally from pair (or triplet, etc.) *potentials*. In particular, even the nn effective pair interaction contains, in principle, all electronic interactions, of arbitrary range. Similar considerations apply, of course, to concentration-dependent $\widehat{E_\alpha}$ interactions.

It may appear curious that the same physical quantity, such as the expectation value of the configurational energy, could be represented equally by series featuring concentration-dependent or -independent interactions. Actually, only the value of the *summed series* matters, not the particular form of the individual coefficients E_α (or $\widehat{E_\alpha}$). In any case, the energy <E> itself surely depends on the average concentration: in the c-independent ECI case, through the correlations ξ_α only, in the c-dependent ECI case, both through the $\widehat{E_\alpha}$ and the cumulants $\widehat{\xi_\alpha}$.

If only effective pair interactions are considered in the c-independent case, then all energetic properties of a binary alloy will be symmetric about the mid-point of the (0,1) concentration interval, at c = 0.5. In actual practice, such perfect symmetry is not observed. It is then necessary to use either multisite ECI's (beyond the pair) in the c-independent case, or, if pair interactions are deemed sufficient, use the c-dependent scheme. The ultimate equivalence of these two approaches can be understood qualitatively as follows: if multisite interactions are included in the expansion then a nn pair energy W_{AB}, say, will have different energies depending upon the configuration of the larger cluster ($W_{ABAAB}\ldots$) that includes it. Thus, in the c-independent scheme, a given pair

"knows about" the composition of its local environment. In the c-dependent scheme, the pair in question "knows about" the average composition of the whole system. In the limit of very large clusters, both schemes are seen to be equivalent.

Cluster expansions would not be of much use if the series did not converge sufficiently rapidly. Unfortunately, there exist, as yet, no rigorous criteria for the convergence of, say, the energy expansions. One has to rely on heuristic arguments or on actual numerical calculations. As a general rule, it is found that the magnitude of pair interactions V_2 (we now adopt this notation, which is simpler than E_{pq}) decreases as the pair spacing increases. It is easy to see why this is so, qualitatively: for large separation between p and q, the energy W_{IJ} is practically proportional to the sum of the "point" energies $W_I + W_J$, since the atom at p hardly "notices" the one at q, and conversely. But if the pair energy is equal to the sum of the corresponding point energies, the linear combination (12) vanishes. Likewise, the magnitude of cluster interactions tends to decrease rapidly as the "size" of the cluster increases: if an atom, A or B, is added to a given cluster α, we have

$$V_{\alpha+1} = \tfrac{1}{2}[V_\alpha(+A) - V_\alpha(+B)]$$

where $V_\alpha(+I)$ denote the ECI for cluster α with an I atom added to it. The addition of one atom to a large cluster will have little effect on the value of $V_\alpha(+A)$ or $V_\alpha(+B)$, so the difference in Eq. (13) will tend to be much smaller than V_α itself.

How are the ECI's to be calculated in practice? The most obvious way of computing ECI's (E_α) is by taking sums and differences of W's, as in Eq. (12). The energies W themselves can be calculated by selecting an arbitrary configuration σ in a finite portion of the crystal (containing N atoms), computing the energy by suitable electronic structure techniques, then repeating the procedure over and over, with different configurations selected at random, keeping that on the chosen α-cluster fixed. It has been shown that convergence is obtained after about 30 configurations [12].

Obviously, the computations are very repetitive, hence lengthy. For that reason, we have used the very efficient tight-binding approximation for the band structure energy of the configurational energy $E(\sigma)$ of each configuration, that of the cluster and that of the outside medium, comprising about 1000 lattice sites. Tight-binding parameters were obtained from LMTO (linear muffin-tin orbital) calculations in the atomic sphere approximation (ASA) for the pure metal elements [13]. Scalar relativistic effects were included along with (in some cases) so-called combined correction terms. Hopping integrals for unlike atomic sites were calculated by taking geometric means. Change in matrix elements of the Hamiltonian upon alloying was taken into account by shifting the on-site energies of the pure elements, the shift being determined self-consistently, along with the location of the Fermi level, by imposing local charge neutrality, a reasonable assumption for transition metal alloys. The resulting Hamiltonian, containing matrix elements from s, p and d orbital contributions, in nn and nnn hopping integrals, was tridiagonalized by using the recursion method [14]. Since this is a real-space method which does not appeal to the Bloch theorem, any non-translationally symmetric configuration can be handled in this way. Actually, taking differences of large numbers, as prescribed by Eq. (12), can be avoided by use of the "orbital peeling" method introduced by Burke [15].

We have called the method just presented the method of *direct configurational averaging* (DCA) [12], since it is based on the exact definition of the ECI's given symbolically in Eq. (5), or more explicitly for pairs in Eqs. (11) and (12). A flow chart of the DCA is shown in Fig. 1. Atomic numbers of the constituent atoms, A, B, C ... are selected, then a lattice is chosen (fcc, bcc, hcp), then tight-binding parameters are obtained by the LMTO method. A cluster of n_α sites is chosen, and is "embedded" in a medium of $N-n_\alpha$ atoms. For a given "medium" configuration (σ'), all configurations of atoms on the sites of the selected cluster are examined, and recursion plus orbital peeling operations are performed for all configurations of the cluster in that particular medium configuration (σ'). Since recursion returns a Hamiltonian in tridiagonal form, the local density of states (LDOS) is obtained as a continued fraction which is continued by use of a quadratic terminator. The whole calculation is repeated for a number of other medium

configurations. All possible 2^N configurations should be thus investigated, obviously an impractical task. Usually, about 20 to 50 configurations suffice. Generally, the average concentration of each configuration turns out to be, as expected for such a large computational region, very close to c = 1/2. Local densities of states for the various configurations are averaged together, and the ECI's are then obtained by integration up to the Fermi level.

The types of clusters for which ECI's have been calculated on fcc lattices are shown in Fig. 2. The first subscript on the V symbol indicates the number of points in the cluster, the second denotes the type of pair (triplet, etc.) envisaged. Values of ECI's calculated for a model system (canonical d-band, number of d electrons for A and B elements equal to 8 and 3, respectively), are plotted in Fig. 3 on a logarithmic scale for interactions normalized by the absolute value of the nn pair $V_{2,1}$. It is seen that convergence is quite rapid, though not necessarily monotonic in pair spacing or cluster "size". In particular, note that the octahedron cluster ECI is almost four orders of magnitude smaller than $V_{2,1}$. It also follows that almost 90% of the ordering energy is already contained in the cluster expansion terminated after the nn pair. By "ordering energy" is meant the expression

$$\Delta E_{ord} = \sum_{\alpha} E_{\alpha} \delta\xi_{\alpha} \tag{14}$$

where

$$\delta\xi_{\alpha} = \xi_{\alpha} - \bar{\sigma}^{n_{\alpha}} \tag{15}$$

is the difference between the α-cluster correlation function (at given T and $\bar{\sigma}$ = 1–2c) and the corresponding one for the fully disordered state, for which multisite correlations are simply powers of the "point" correlation, or average spin. ΔE in Eq. (14) thus has the form of the difference between the energy of the (partially) ordered configuration, characterized by its ξ_{α} correlations,

and the energy of the random state. It follows that, in most cases, the most important role played by higher ECI's (beyond $V_{2,1}$) is that of lifting structural degeneracies, i.e., of insuring that the correct ordered superstructure, or ground state, is obtained. This crucial aspect of the calculation, that of predicting ground states, is examined next.

4. Ground States of Order

Predicting, for a given binary system, which intermetallic structures will have lowest energy, for all concentrations, at zero Kelvin, is an impossible task. Fortunately, most intermetallics of interest are superstructures of either fcc, bcc or hcp. Then, the problem of determining the lowest-energy *superstructures* of a given lattice is a simpler one which, in favorable cases, can be solved exactly. Each lattice must of course be handled separately: the ECI's calculated on different lattices will have different values. As for other intermetallic compounds, those which are *not* superstructures, they must be treated differently: for these "interloper" phases, their total energies must be calculated directly by appropriate electronic structure codes and compared to other, possibly competitive structures.

Eq. (4), written for the energy $E(\sigma)$, is the one to minimize, but it must first be rewritten in a more convenient form. Many of the clusters (α) appearing in the summation are equivalent through the space group symmetry operations of the underlying lattice. The set of such clusters equivalent to a given one by symmetry is known as the orbit of the given cluster. Each distinct orbit (or its generating cluster) will be denoted by the index j. The total number of clusters in orbit j is then the total number of lattice translational symmetry operations times the number of equivalent clusters per lattice point, or multiplicity m_j. Let us also denote the "empty cluster" by the index j = 0. Then, the energy of a given stoichiometric superstructure, per lattice point, is, by Eq. (6), given by the linear form

$$e = e_0 + \sum_{j=1}^{J} m_j E_j \xi_j \tag{16}$$

where the brackets have been removed from $< e >$ since, at absolute zero of temperature, the expectation value is just the energy of the perfect structure. The variables ξ_j here are not strictly ensemble averages, but "orbit averages" of cluster functions; such averaging process must be taken into account since the symmetry of the ordered superstructure is generally lower than that of the parent lattice. The summation in Eq. (16) extends from the "point" cluster to some maximal cluster(s), denoted by the index J.

Simply minimizing the linear function (16) with given ECI's E_j will not do since the parameters ξ_j must describe a real structure, or mixture of structures, on the lattice. Hence, a number of constraints (i.e., linear inequalities) on the domain of ξ_j must be imposed. The required constraints are usually derived from considerations of clusters (see Refs. [16] and [17] and references cited therein), but the most straightforward method is probably that suggested by Sanchez and the present author [18] and described fully, for the case of pair interactions, by Finel [17] and in a recent review [19]. The handling of combinatorics of large clusters was treated even more recently in the Ph.D. dissertation of G. Ceder [20] and a more detailed application to the Pd-V system is presented elsewhere [21].

Briefly, the idea is the following: denote the probability of finding a given cluster, say a nearest-neighbor triangle of lattice points (equilateral triangle in fcc) populated by atoms in a certain configuration ($\sigma \equiv$ AAA, AAB, ...) by the symbol $x_j(\sigma)$. This probability, or "dressed" cluster concentration, being a function of configuration, can be expanded in a set of cluster functions, as in Eq. (4). For simplicity, let distinct configurations on a given cluster be labeled by the index k. For the maximal cluster J, the concentrations of various configurations k are then given by [22]:

$$x_j(\sigma_k) \;=\; \rho_J^o\Big(1 + \sum_{j=1}^{J} C_{kj}\xi_j\Big) \tag{17}$$

where ρ_J^o is a normalization factor given by the reciprocal of the number of configurations on the cluster, i.e., 2^{-J}. The summation is over all subclusters j of the maximal cluster J and the coefficients C_{kj}, calculated by means of Eq. (2), are elements of a rectangular matrix, the so-called *configuration matrix* (or C-matrix). Often, more than one "maximal cluster" is used, J, J', J", ..., neither one being a subcluster of any other.

Since the x_j are probabilities, their values must be constrained to lie between 0 and 1. Then, only the lower constraint needs to be considered, since the upper one is guaranteed by the fact that cluster averages lie between –1 and +1. Hence, from Eq. (17), we must have, for all maximal clusters, and for all cluster configurations k,

$$\sum_j C_{kj} \xi_j \geq -1 \quad . \tag{18}$$

These linear inequalities define a convex region in multidimensional ξ-space, the so-called configurational polyhedron, which contains all realizable configurations on the lattice. The determination of ground states then consists of minimizing the energy (objective) function (16), under the constraint of inequalities (18). This is a standard problem in linear programming and can be solved by the simplex algorithm, but only when the ECI's are calculated in the c-independent case. It follows that the vertices of the configuration polyhedron are the solutions sought, i.e, the ordered ground state superstructures, different vertices corresponding to different stoichiometries. One must then construct the crystal superstructure corresponding to the correlations ξ, which are the coordinates of the vertex to which the linear programming algorithm has converged. This is a non-trivial problem; in fact, there are cases for which the ξ-coordinates of a vertex do not correspond to a constructible crystal structure.

The C-matrix, which has more rows (configurations k) than columns (subcluster types j) contains all the geometric properties of the problem, and is used to transfer that information (lattice

type, largest cluster(s), subclusters, symmetry equivalence) to both ground state and CVM codes. Unfortunately, the number of (sub)clusters and the number of configurations tend to increase exponentially with the number of points in the largest cluster retained in the energy (or entropy) approximation chosen. For example, in the 13-, 14-point fcc approximation (central lattice point and its twelve nearest neighbors, fcc cube itself), there are 742 distinct clusters, 554 configurations on the 14-point cluster and 288 on the 13-point cluster. Hence the C-matrix has 842×742 elements! Clearly, the enumeration of all variables and constraints must be obtained by a suitable computer algorithm based on group theoretic considerations. One such algorithm has recently been developed [20].

5. Phase Diagrams

When temperature is brought into the picture, so must its conjugate "extensive" quantity, the entropy S, be included. Here, we shall be concerned only with configurational entropy. If equilibria between ordered structures on the same reference lattice only are considered, then the change of vibrational entropy upon phase transition is probably quite small compared to the configurational contribution. Thermal expansion will also be neglected since, over the range of temperatures of interest for crystalline phase equilibria, the lattice parameter dilatations are expected to have little influence on the values of the calculated ECI's. Hence, the appropriate thermodynamic function to be minimized at equilibrium is the Helmholtz free energy $F = E - TS$.

The basic idea of the CVM is to express the configurational entropy as an analytic function of the cluster concentrations $x_j(\sigma)$ defined in the previous section. Kikuchi [1] showed that the configurational entropy per lattice point could be expressed as

$$S = k_B \sum_j \gamma_j \sum_k x_j(\sigma_k) \ln x_j(\sigma_k) \tag{19}$$

where k_B is Boltzmann's constant, $x_j(\sigma_k)$ is the concentration, or frequency of occurrence at equilibrium of cluster of type j in configuration σ_k, and γ_j are integers which depend on the nature of the (sub)lattice and on the cluster approximation used. The first summation in Eq. (19) is in principle, over all clusters, the second one over all configurations of the cluster considered. Cluster concentrations x_j and correlation functions ξ are linearly related by the configuration matrix C, as in Eq. (17). The configurational free energy can then be written as an implicit function of the (independent) correlations as $F = F(\xi)$, collectively. The variational principle is now invoked to claim that the equilibrium free energy is the one obtained by minimizing $F(\xi)$ with respect to the multisite correlation retained in the approximation. The choice of clusters which produce satisfactory approximations is discussed at some length by Finel [17].

Phase diagram calculations proceed as indicated schematically in the flow diagram of Fig. 4. The DCA flow diagram of Fig. 1 ended with the all-important ECI's which provide the link between quantum and statistical mechanical calculations. The CVM flow diagram of Fig. 4 starts when Fig. 1 leaves off. Knowledge of the configuration matrix and of the ECI's determines the ground states, hence the ordered phases which are expected to play a role in the system under consideration, for each of the lattices. For each phase, the free energy is minimized, and the equilibrium F is plotted as a function of T and c. All lattices must be handled in this way (in Fig. 4, see arrow marked "Another Lattice" returning the calculation to the lattice selection box of Fig. 1). Finally, domains of existence of stable (and metastable) phases are determined by constructing common tangents to the relevant equilibrium free energy curves, according to standard classical thermodynamic procedure.

Such calculations are extremely valuable to perform even when the phase diagram has already been determined from experimental measurements. The calculated diagram gives much more than a picture, or map of stable equilibria: numerical values of energies of cohesion, formation, order have been calculated, along with equilibrium lattice parameters, elastic moduli, entropies, free energies. It is also possible to deduce, from the calculations leading to the phase diagram, information concerning states of long- and short-range as a function of T and c, and other

parameters of interest. In addition, it becomes possible to understand the physical why and wherefore of a phase diagram: why certain phases coexist, why they have certain domains of existence.

6. Application to Pd-Rh-V Systems

The tight-binding approximation is expected to give satisfactory results for transition metals, so let us take, by way of example, the three metals Pd, Rh and V. Here, only the fcc reference lattice is considered. The c-independent scheme was adopted for the binaries Pd-V and Pd-Rh, which means, practically, that DCA calculations were performed at alloy compositions very close to 0.5. A volume correction was introduced by assuming that average atomic volumes varied linearly with concentration. Atomic volumes of pure elements were calculated by minimizing the energy of Pd, Rh and V obtained by the LMTO-ASA. The tight-binding parameters of these elements, to be used in binary alloy calculations, were obtained from the LMTO at volumes corresponding to the 0.5 alloy concentration.

For each of the three binary systems, first through fourth-neighbor pair interactions were calculated, as well as several triplet and quadruplet interactions. ECI's thus calculated for Pd-V and Pd-Rh are plotted in Figs. 5a and b respectively (filled circles). Lines are mere guides to the eye. It is seen that, as expected, convergence to very small ECI values is quite rapid. For comparison, Figs. 5a and b also show (open circles, dashed line) ECI's calculated by other first-principles methods, the KKR-CPA-GPM for Pd-V [22], and the inversion (or Connolly-Williams) method, featuring LAPW calculations for Pd-Rh [23]. It is seen that, in both cases, the agreement is very good between the TB-DCA and the calculations based on more elaborate electronic structure techniques.

Having obtained numerical values of the ECI's, we can now search for fcc-based superstructure ground states, according to the methods described in Section 4. Pd-V calculations are described in more detail elsewhere [21]; Fig. 6a summarizes the results. All vertices obtained by the linear programming method were found to be "constructible" and are shown, with their

respective structures and formation energies, as filled circles lying along the *convex hull* (full polygonal line) in Fig. 6a. The dashed curve in this figure represents the formation energy of the fully disordered state, obtained by replacing actual correlations by powers of the "point" correlation, as explained in connection with Eq. (15). By "formation energy" we mean the total energy of a superstructure, here at zero Kelvin, compared to the non-interacting mixture of pure (fcc) elements at the same concentration. Of course, the equilibrium structure of pure V is bcc, so that the diagram of Fig. 6a is incomplete; one would have to perform the same analysis on the bcc lattice, for V, Pd and all its ground state superstructures, followed by construction of the *lowest* convex hull. This has not yet been done, but comparison of the Pd side of Fig. 6a with experimental evidence is quite encouraging: the DO_{22}-type structure is indeed the one observed to be the stable one for VPd_3, and the $MoPt_2$-type structure is the observed one for VPd_2. The Ni_4Mo-type structure ($D1_a$) is not observed in this system, but its representative point is seen to lie in Fig. 6a practically on the tie line between pure fcc Pd and DO_{22}. If the energy of "VPd_4" were pushed up ever so slightly, it would cease to appear in the ground state diagram. In the actual V-Pd system, a two-phase region straddles the 50-50 composition, and therefore masks the possible appearance of the predicted $L1_0$ fcc superstructure.

Ground state results for V-Rh are shown similarly in Fig. 6b. In this case, at the AB_3 composition, it is the $L1_2$ structure which is stable, in agreement with experiment, rather than the DO_{22} of VPd_3. Also, in V-Rh, there are no predicted VRh_2 and VRh_4 stable superstructures, again in agreement with experiment. It follows that the fcc portion of the V-Rh system belongs to the <100> family of superstructures, and V-Pd to the $<1\frac{1}{2}0>$ family, the bracketed expression indicating the Miller indices of the concentration wave corresponding to the ordering instability [16].

The ground state search for Pd-Rh has been performed as well, but the results are trivial: since the nn effective pair interaction is large and *negative*, phase separation rather than ordering is expected, so that the two ground states are just pure fcc Pd and Rh. For this system, however, we have used the CVM to calculate a phase diagram according to the methods described in Section 5.

Only nn and nnn pair interactions were used in the energy expansion. The calculated unmixing boundary (dashed line) is compared in Fig. 7 with the experimentally determined miscibility gap (unbroken line). The excellent agreement is partly due to the fact that the tight-binding parameters for the DCA calculations were calculated from the LMTO at the average atomic volume obtained for the chosen concentration by interpolating linearly between experimental values of the atomic volumes of pure Pd and Rh.

The fact that DCA calculations provide the correct ordering and phase separation trends for the three fcc-based binaries V-Pd, V-Rh and Pd-Rh gives us confidence to tackle the V-Pd-Rh ternary itself. In this preliminary study, ternary ECI's were calculated for first through fourth nn pairs in the c-dependent scheme; otherwise artificial symmetries in the concentration dependence of the energy would develop due to the neglect of multiplet interactions (see Section 3). The formation energy of the completely disordered fcc state is plotted as shaded contours in the V-Pd-Rh Gibbs triangle in Fig. 8. For a narrow strip along the Pd-Rh binary, the energy is positive (phase separation tendency) whereas it is negative (ordering tendencies) for all other concentrations (see vertical energy scale in Fig. 8). One may not conclude, however, that ordering will be preferred at almost all ternary concentrations: it is necessary, at the very least, to perform a stability analysis on the disordered state which, for ternary (and higher) systems is not as straightforward as it is for binaries. Consider, for example, the central composition of the Gibbs triangle. At that point, the contours indicate that the energy surface is saddle-shaped, with negative curvature along directions roughly parallel to the Pd-Rh binary. An instability toward phase separation into Pd-rich and Rh-rich (possibly ordered) solutions is therefore to be expected [16,24].

It is also instructive to examine separately the concentration dependence of the independent Pd-Rh, Pd-V and Rh-V pair interactions. Values of these nn pair interactions are plotted individually on three Gibbs triangles in Fig. 9. The pairs retain their respective signs over the whole composition ranges: negative for Pd-Rh (light shading) positive for the other two (heavy shading). These signs are such as to place the Pd-Rh-V system in category II of Meijering's

diagram is expected to show, as main feature, a miscibility gap extending into the ternary from the Pd-Rh side, without touching the other two binaries.

7. Conclusion

The cluster method has become the preferred technique for the study of crystalline alloys, binary, ternary, stable, metastable, ordered, disordered. The orthonormal expansion is in principle exact, and its convergence properties make it an indispensable tool for the theoretical study of alloys. The DCA is the most straightforward application of the cluster method, and its TB-LMTO formulation has been shown to provide excellent quantitative results for transition metal alloys, in particular for fcc-based Pd-Rh-V binary and ternary systems. Much work remains to be done, but we can already foresee the impact that a truly reliable first-principles thermodynamic theory will have on predicting properties of materials.

Acknowledgments

This work was supported by the Director, Office of Energy Research, Office of Basic Energy Sciences, Materials Sciences Division of the U. S. Department of Energy under Contract No. DE-AC03-76SF00098. DdF is greatly indebted to Ryoichi Kikuchi, who introduced him to the CVM, and to many students and collaborators, past and present, among them M. Asta, G. Ceder, H. Dreyssé, T. Mohri and J. M. Sanchez, who are responsible for the main results reported in this paper.

References

[1] R. Kikuchi, Phys. Rev. 81, 988 (1951).

[2] C. M. van Baal, Physica (Utrecht) 64, 571 (1973).

[3] D. de Fontaine and R. Kikuchi, NBS Special Publication 496, 1978, p. 999.

[4] J. M. Sanchez and D. de Fontaine, Phys. Rev. B 17, 2926 (1978).

[5] J. M. Sanchez and D. de Fontaine, Phys. Rev. B 21, 216 (1980).

[6] J. M. Sanchez and D. de Fontaine, Phys. Rev. B 25, 1759 (1982).

[7] T. Mohri, J. M. Sanchez and D. de Fontaine, Acta Metall. 33, 1171 (1985).

[8] C. Sigli and J. M. Sanchez, Acta Metall. 33, 243 (1985).

[9] J. M. Sanchez, F. Ducastelle and D. Gratias, Physica A 128, 334 (1984).

[10] M. Asta, C. Wolverton, D. de Fontaine and H. Dreyssé, Phys. Rev. B 44, 4907, (1991).

[11] C. Wolverton, M. Asta, H. Dreyssé and D. de Fontaine, Phys. Rev. B 44, 4914 (1991).

[12] H. Dreyssé, A. Berera, L. T. Wille and D. de Fontaine, Phys. Rev. B 39, 2442 (1989).

[13] O. K. Andersen, O. Jepsen and M. Sob, in M. Youssouf (ed.), Electronic Band Structure and Its Applications, Springer, Berlin, 1987, pp. 1-56.

[14] R. Haydock, Solid State Phys. 35, 215 (1980).

[15] N. R. Burke, Surf. Sci. 58, 349 (1976).

[16] D. de Fontaine, "Configurational Thermodynamics of Solid Solutions", in H. Ehrenreich, F. Seitz and D. Turnbull (eds.), Solid State Physics, Vol. 34, Academic Press, 1979, pp. 73-294.

[17] A. Finel, "Contribution à l'Etude des Effets d'Ordre dans le Cadre du Modèle d'Ising: Etats de Base et Diagrammes de Phase", doctoral dissertation, Université Pierre et Marie Curie, Paris, 1987 (unpublished).

[18] J. M. Sanchez and D. de Fontaine, "Theoretical Prediction of Ordered Superstructures in Metallic Alloys", in Michael O'Keeffe and Alexandra Navrotsky (eds.), Structure and Bonding in Crystals, Vol. II, Academic Press, 1981, pp. 117-132.

[19] G. Inden and W. Pitsch, "Atomic Ordering", in Peter Haasen (ed.), Materials Science and Technology, Vol. 5, VCH Press, Weinheim, 1991, pp. 497-552.

[20] Gerbrand Ceder, "Alloy Theory and Its Applications to Long Period Superstructure Ordering in Metallic Alloys and High Temperature Superconductors", Ph.D. dissertation, University of California, Berkeley, 1991 (unpublished).

[21] C. Wolverton, G. Ceder, D. de Fontaine and H. Dreyssé, Phys. Rev. B 45, 13105 (1992).

[22] P. Turchi, G. Stocks, W. Butler, D. Nicholson and A. Gonis, Phys. Rev. B 37, 5982 (1988).

[23] Z. W. Lu, S.-H. Wei, A. Zunger and L. G. Ferreira, Solid State Commun. 78, 583 (1991).

[24] D. de Fontaine, J. Phys. Chem. Solids 33, 297 (1972); 34, 1285 (1973).

[25] J. L. Meijering, Philips Res. Report 5, 333 (1950); 6, 183 (1951).

Figure Captions

Fig. 1. Flow chart of direct configurational averaging (DCA) method.

Fig. 2. Clusters of fcc lattice points used in the DCA calculations.

Fig. 3. Convergence of effective cluster interactions (ECI) as a function of pair separation and cluster types. As in Fig. 2, subscripts on the V symbols (ECI's) indicate, first, the number of points in the cluster, then the pair spacing or cluster type.

Fig. 4. Flow chart for CVM phase diagram calculations. Free energy curves and phase diagram are schematic only.

Fig. 5. Effective cluster interactions calculated by the DCA (filled circles) and by other electronic structure methods (empty circles): (a) Pd-V, (b) Pd-Rh systems.

Fig. 6. Formation energies of fcc ground state superstructures for (a) Pd-V, (b) Rh-V systems. Dashed curve is for formation energy of fully disordered state.

Fig. 7. Pd-Rh phase diagram with calculated and experimentally determined miscibility gap.

Fig. 8. Formation energy of the completely random system Pd-Rh-V. The largest negative formation energies are seen to occur not at equiatomic composition, but rather at two positions near the equiatomic binary Rh-V and Pd-V systems.

Fig. 9. Effective pair interactions for the ternary system Pd-Rh-V. Each of the three types of distinct pair interactions is calculated individually over the entire composition space of the ternary alloy. Negative values of the interaction (light shading) indicate phase separating tendencies. Strong ordering tendencies are given by positive values of the interaction (dark shading).

DCA

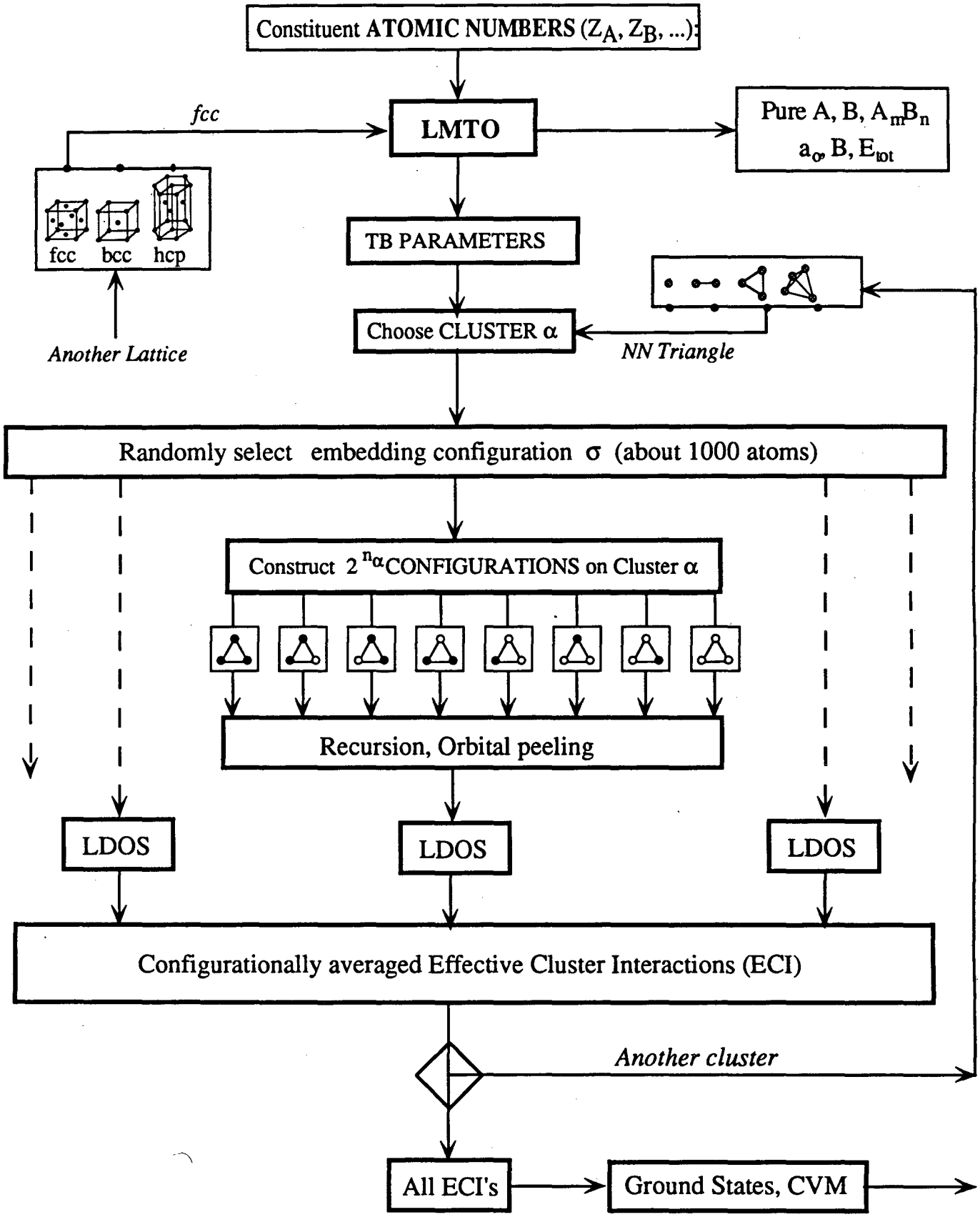
Constituent ATOMIC NUMBERS (Z_A, Z_B, ...)
fcc
LMTO
Pure A, B, A_mB_n
a_o, B, E_{tot}
fcc bcc hcp
TB PARAMETERS
Another Lattice
Choose CLUSTER α
NN Triangle
Randomly select embedding configuration σ (about 1000 atoms)
Construct 2^{n_α} CONFIGURATIONS on Cluster α
Recursion, Orbital peeling
LDOS
LDOS
LDOS
Configurationally averaged Effective Cluster Interactions (ECI)
Another cluster
All ECI's
Ground States, CVM

Fig. 1

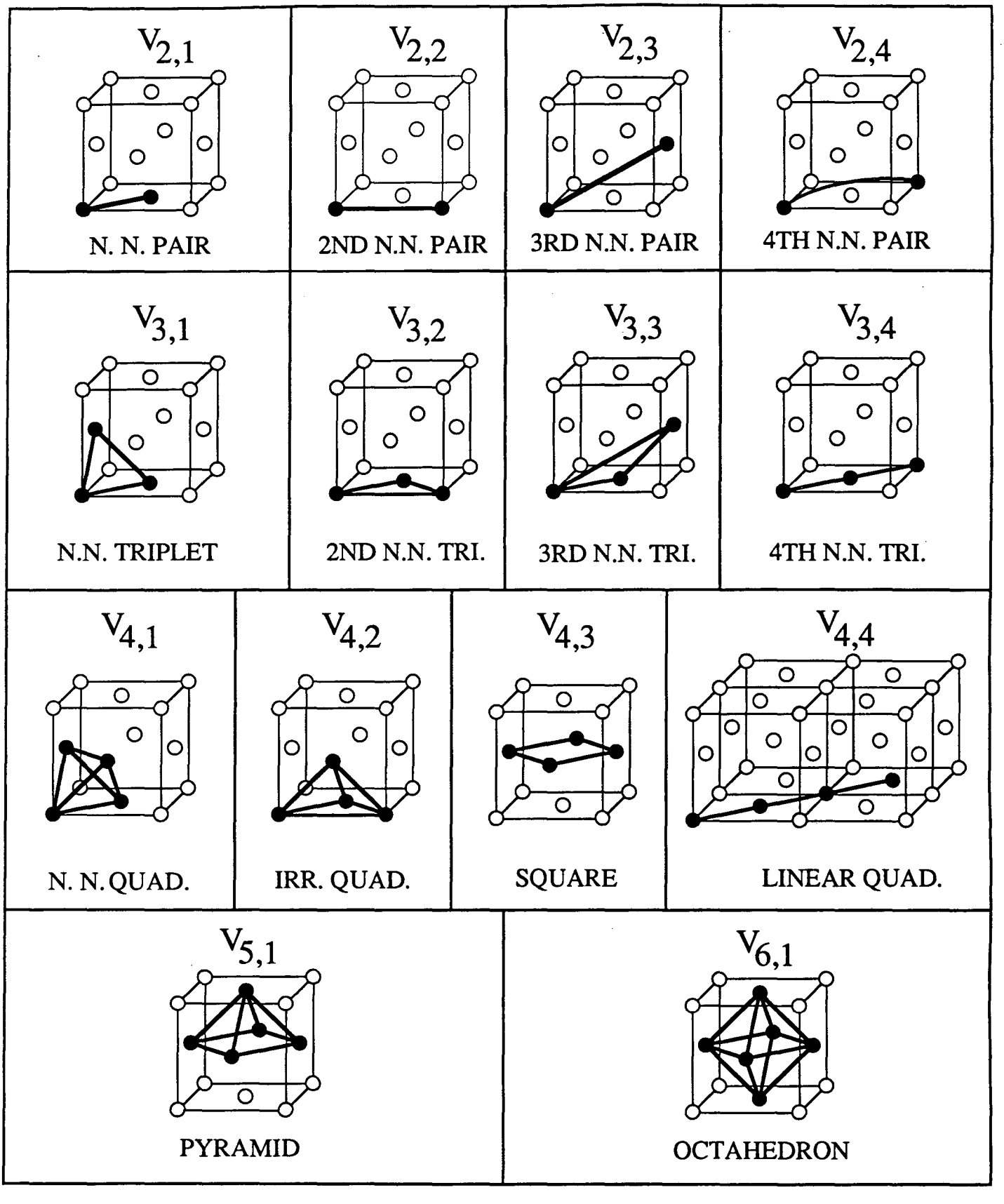
$V_{2,1}$
N. N. PAIR
$V_{2,2}$
2ND N.N. PAIR
$V_{2,3}$
3RD N.N. PAIR
$V_{2,4}$
4TH N.N. PAIR
$V_{3,1}$
N.N. TRIPLET
$V_{3,2}$
2ND N.N. TRI.
$V_{3,3}$
3RD N.N. TRI.
$V_{3,4}$
4TH N.N. TRI.
$V_{4,1}$
N. N. QUAD.
$V_{4,2}$
IRR. QUAD.
$V_{4,3}$
SQUARE
$V_{4,4}$
LINEAR QUAD.
$V_{5,1}$
PYRAMID
$V_{6,1}$
OCTAHEDRON

Fig. 2

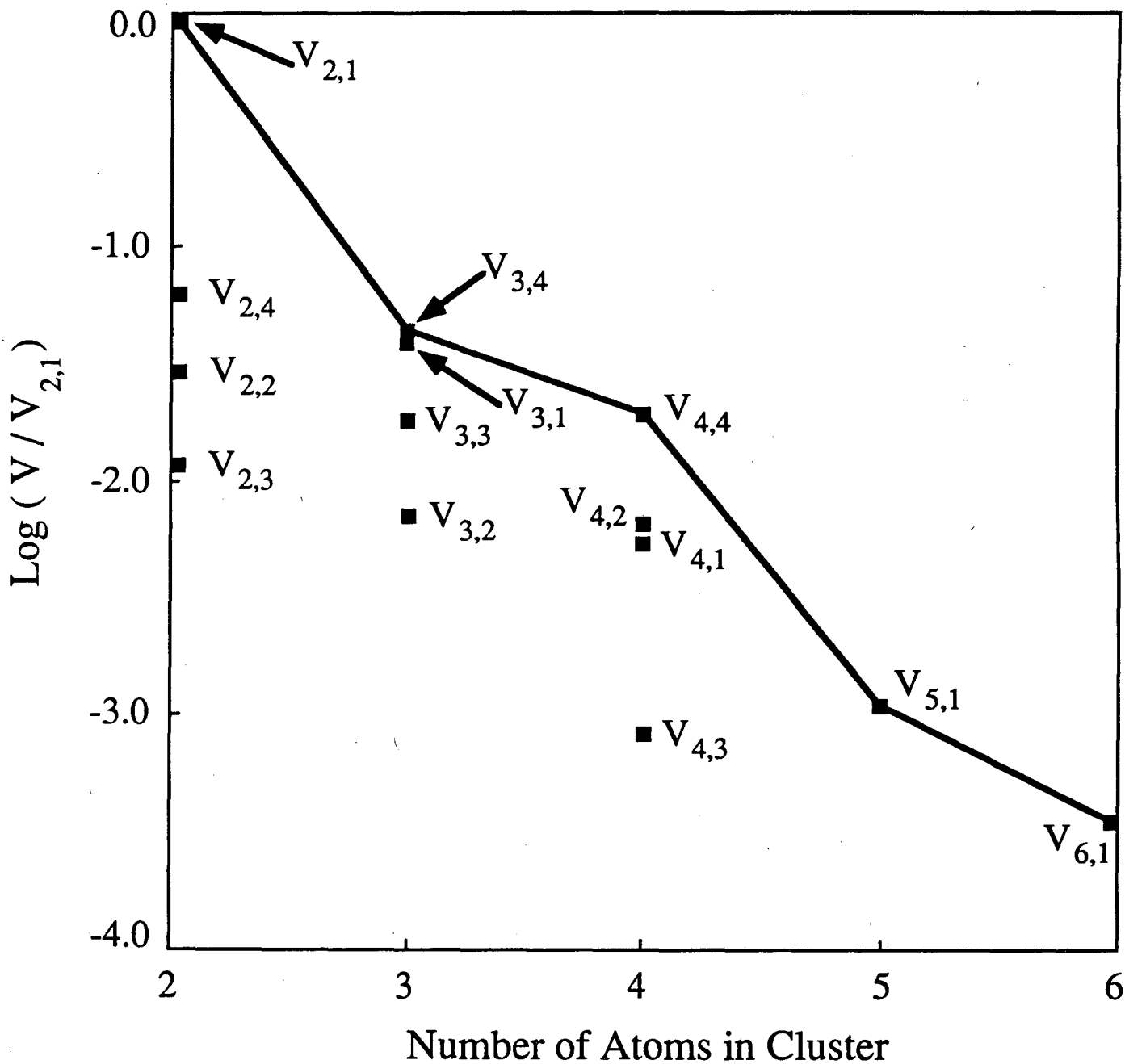
0.0
-1.0
-2.0
-3.0
-4.0
Log (V / V2,1)
2
3
4
5
6
Number of Atoms in Cluster
V2,1
V3,4
V3,1
V4,4
V5,1
V6,1
V2,4
V2,2
V2,3
V3,3
V3,2
V4,2
V4,1
V4,3

Fig. 3

CVM

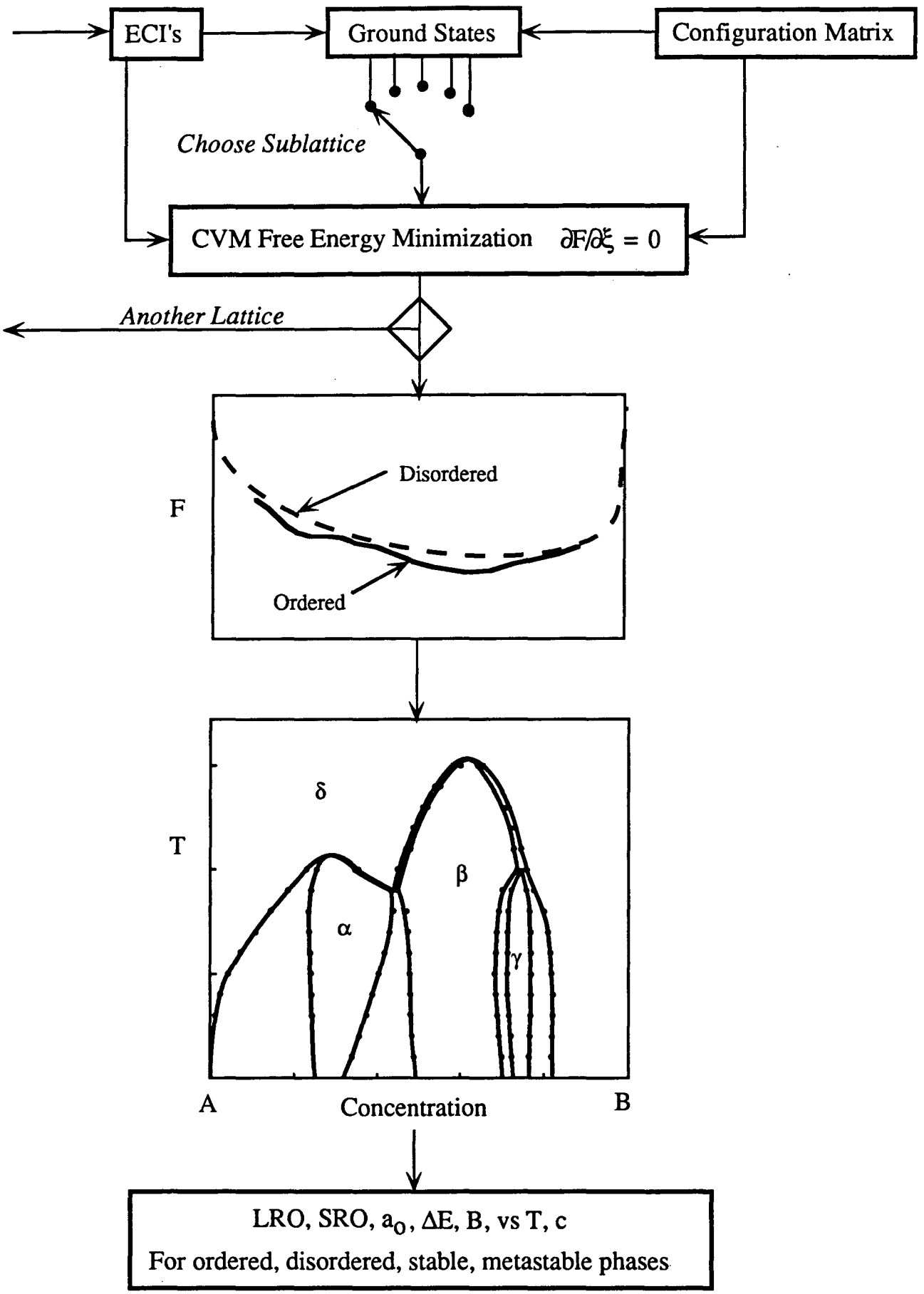
ECI's
Ground States
Configuration Matrix
Choose Sublattice
CVM Free Energy Minimization ∂F/∂ξ = 0
Another Lattice
F
Disordered
Ordered
T
δ
β
α
γ
A
Concentration
B
LRO, SRO, a0, ΔE, B, vs T, c
For ordered, disordered, stable, metastable phases

Fig. 4

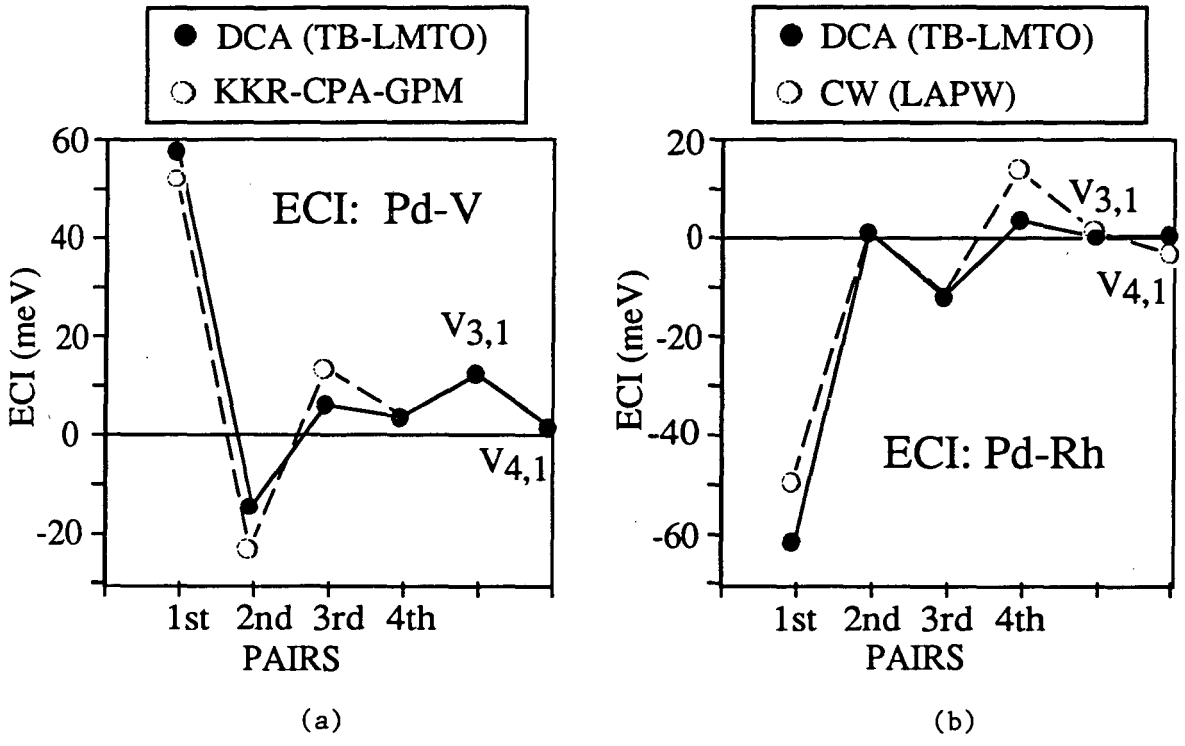
DCA (TB-LMTO)
KKR-CPA-GPM
ECI: Pd-V
ECI (meV)
60
40
20
0
-20
V3,1
V4,1
1st
2nd
3rd
4th
PAIRS
(a)
DCA (TB-LMTO)
CW (LAPW)
ECI: Pd-Rh
ECI (meV)
20
0
-20
-40
-60
V3,1
V4,1
1st
2nd
3rd
4th
PAIRS
(b)

Fig. 5

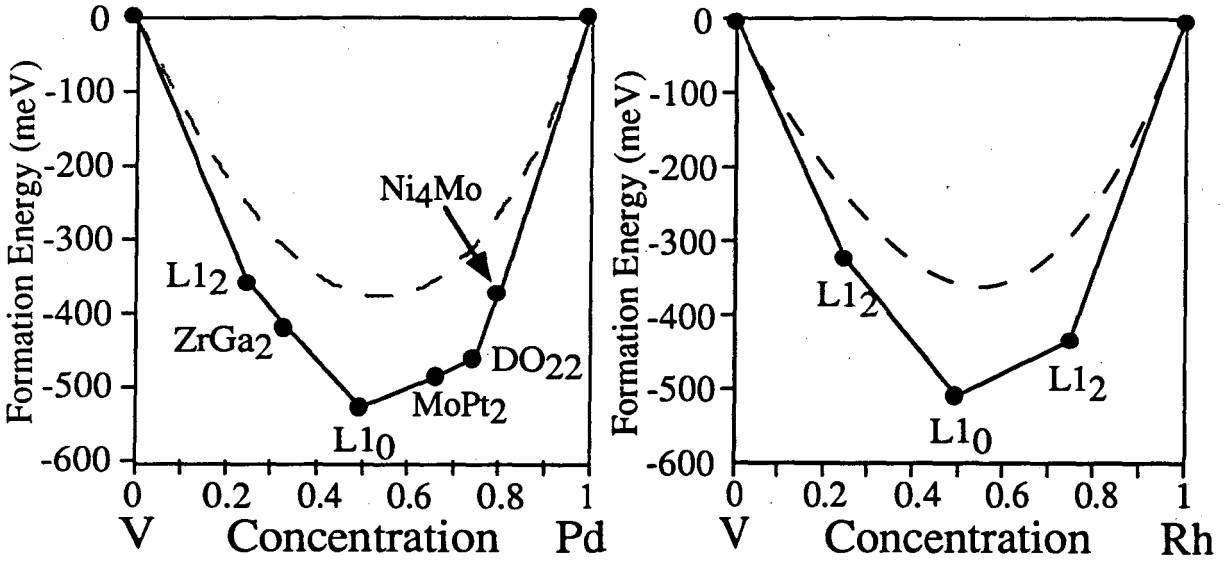
0
-100
-200
-300
-400
-500
-600
Formation Energy (meV)
Ni4Mo
L12
ZrGa2
DO22
MoPt2
L10
0
0.2
0.4
0.6
0.8
1
V
Concentration
Pd
0
-100
-200
-300
-400
-500
-600
Formation Energy (meV)
L12
L12
L10
0
0.2
0.4
0.6
0.8
1
V
Concentration
Rh

(a) (b)

Fig. 6

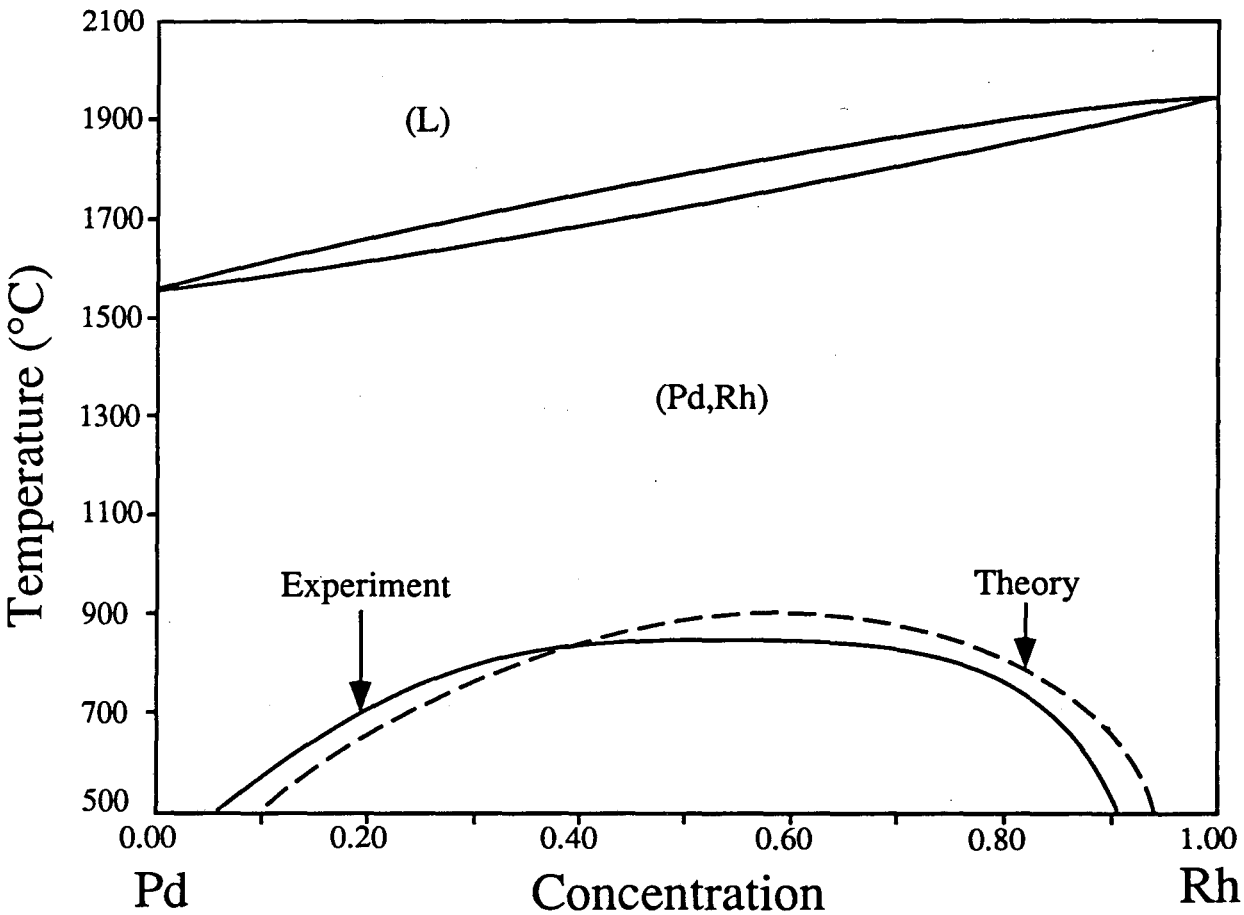
2100
1900
1700
1500
1300
1100
900
700
500
Temperature (°C)
(L)
(Pd,Rh)
Experiment
Theory
0.00
0.20
0.40
0.60
0.80
1.00
Pd
Concentration
Rh

Fig. 7

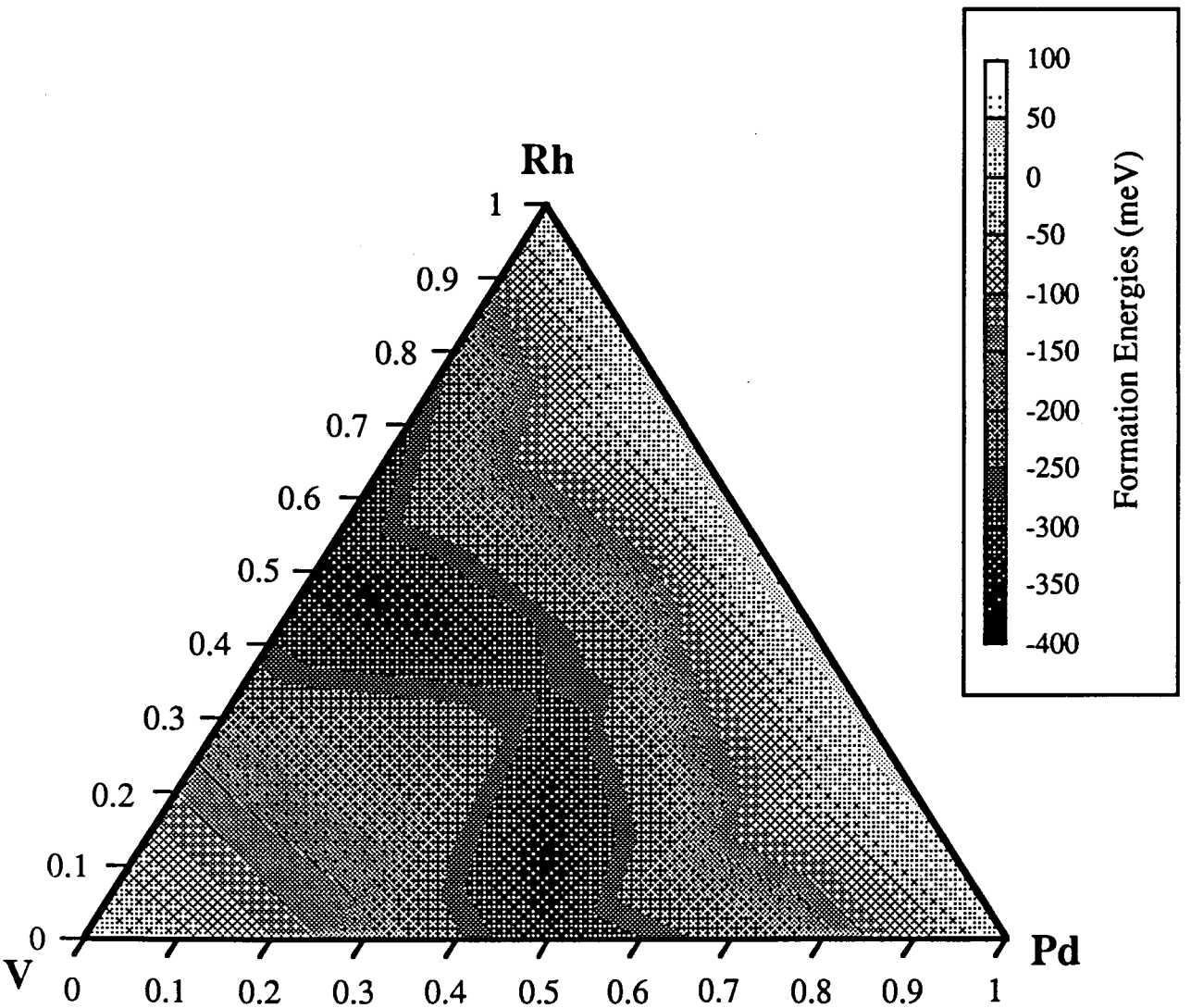
Rh
Pd
V
0
0.1
0.2
0.3
0.4
0.5
0.6
0.7
0.8
0.9
1
100
50
0
-50
-100
-150
-200
-250
-300
-350
-400
Formation Energies (meV)

Fig. 8

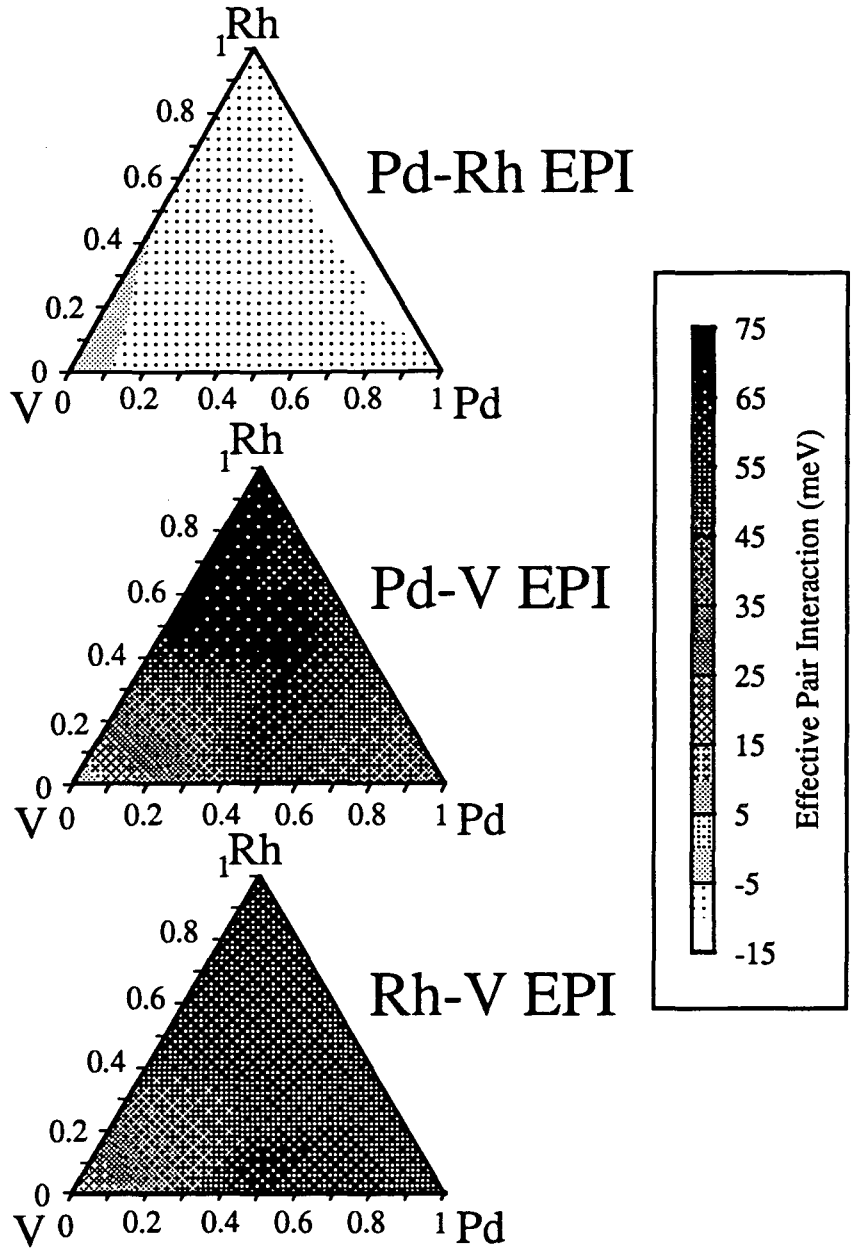
Rh
Pd-Rh EPI
Pd-V EPI
Rh-V EPI
V
Pd
0
0.2
0.4
0.6
0.8
1
75
65
55
45
35
25
15
5
-5
-15
Effective Pair Interaction (meV)

Fig. 9

LAWRENCE BERKELEY LABORATORY
UNIVERSITY OF CALIFORNIA
TECHNICAL INFORMATION DEPARTMENT
BERKELEY, CALIFORNIA 94720